Transient Kinetic Studies of Heme Reduction in Escherichia coli Nitrate Reductase A (NarGHI) by Menaquinol †

3 AUTHORS:

Zhongwei Zhao
Capital Medical University
20 PUBLICATIONS   558 CITATIONS

SEE PROFILE

Richard Adrian Rothery
University of Alberta
74 PUBLICATIONS   2,350 CITATIONS

SEE PROFILE

Joel H Weiner
University of Alberta
191 PUBLICATIONS   6,815 CITATIONS

SEE PROFILE

Transient Kinetic Studies of Heme Reduction in *Escherichia coli* Nitrate Reductase A (NarGHI) by Menaquinol[†]

Zhongwei Zhao, Richard A. Rothery, and Joel H. Weiner*,‡

CIHR Membrane Protein Research Group, Department of Biochemistry, 474 Medical Sciences Building, University of Alberta, Edmonton, Alberta T6G 2H7, Canada

ABSTRACT: We have studied the transient kinetics of quinol-dependent heme reduction in *Escherichia coli* nitrate reductase A (NarGHI) by the menaquinol analogue menadiol using the stopped-flow method. Four kinetic phases are observed in the reduction of the hemes. A transient species, likely to be associated with a semiquinone radical anion, is observed with kinetics that correlates with one of the phases. The decay of the transient species and the formation of the second reduction phase of the hemes can be fitted to a double-exponential equation giving similar rate constants, $k_1 = 9.24 \pm 0.9$ s^{-1} and $k_2 = 0.22 \pm 0.02$ s^{-1} for the decay of the transient species, and $k_1 = 9.23 \pm 0.9$ s^{-1} and $k_2 = 0.22 \pm 0.02$ s^{-1} for the formation of the reduction phase. The quinol-binding-site inhibitors 2-*n*-heptyl-4-hydroxyquinoline-*N*-oxide (HOQNO) and stigmatellin have significant and different inhibitory effects on the reduction kinetics. The kinetics of heme reduction in NarI expressed in the absence of the NarGH catalytic dimer (NarI(ΔGH)) exhibits only two kinetic phases, and the decay of the transient species also correlates kinetically with the second reduction phase of the hemes. We have also studied nitrate-dependent heme reoxidation following quinol-dependent heme reduction using a sequential stopped-flow method. HOQNO elicits a much stronger inhibitory effect than stigmatellin on the reoxidation of the hemes. On the basis of our results, we propose schemes for the mechanism of NarGHI reduction by menaquinol and reoxidation by nitrate.

During anaerobic growth, *Escherichia coli* develops specialized respiratory chains that consist of a group of primary dehydrogenases, an intermediate electron carrier (menaquinol, MQH$_2$; ubiquinol, UQH$_2$; or demethyl-menaquinol, DMQH$_2$), and a series of terminal reductases (*1*). Nitrate reductase A (NarGHI),[1] one of these terminal reductases, catalyzes MQH$_2$ or UQH$_2$ oxidation accompanied by proton release at the periplasmic side of the membrane, and nitrate reduction accompanied by consumption of protons at the cytoplasmic side of the membrane (*2−4*). NarGHI is a heme-containing iron−sulfur molybdoenzyme and consists a catalytic subunit (NarG, 140 kDa) having a molybdo-bis-(molybdopterin guanine dinucleotide) cofactor (Mo-bisMGD) at its active site (*5, 6*), an electron-transfer subunit (NarH, 58 kDa) with four iron−sulfur clusters (three [4Fe-4S] clusters and one [3Fe-4S] cluster) (*5, 7, 8*), and a membrane anchor subunit (NarI, 26 kDa) with two hemes (one, heme b_H, has a higher midpoint potential E_m of +120 mV, and the other, heme b_L has a lower midpoint potential E_m of +20

mV) (*9−11*). In the overall structure of the enzyme, the NarG and NarH subunits are anchored as a NarGH catalytic dimer to the inner surface of the cytoplasmic membrane by the NarI subunit.

The electron-transfer pathway in NarGHI has been investigated using biochemical and biophysical methods (for reviews, see refs *4, 12, 13*). Based on available data, a plausible electron-transfer pathway begins at a MQH$_2$/UQH$_2$ binding site (Q-site) located toward the periplasmic side of the NarI subunit (*14*). Electrons from quinol oxidation are transferred from this site, via hemes b_L and b_H, the [3Fe-4S] cluster, and some of the remaining [4Fe-4S] clusters located in the NarH subunit, to the Mo-bisMGD cofactor of the NarG subunit in the catalytic dimer (*5, 10*). Based on the presence of an N-terminal Cys group within the sequence of the NarG subunit, it is also possible that there is an additional [4Fe-4S] cluster coordinated by this subunit (*15, 16*), although no experimental data exist to date to support its presence (*6*). Overall, as proposed by Iwata and co-workers (*17*), protons are released into the periplasm by quinol oxidation and are consumed in the cytoplasm by nitrate reduction.

Although some steady-state kinetic studies (*18, 19*) and spectroscopic studies (*14, 20*) on the interaction of quinol with nitrate reductase from *E. coli* have been carried out, a transient kinetic study on the initial fast reactions has not been reported. It was proposed from a steady-state kinetic study that a two-site enzyme-substitution (ping-pong) mechanism could be applied to describe the nitrate-dependent quinol oxidation catalized by *E. coli* nitrate reductase (*18*). It has been observed in conventional spectroscopy studies

* To whom correspondence should be addressed. Telephone: (780) 492-2761. Fax: (780) 492-0886. E-mail: joel.weiner@ualberta.ca.
‡ J. H. W. is a Canadian Research Chair in Membrane Biochemistry.

[1] Abbreviations: DmsABC, *Escherichia coli* dimethyl sulfoxide reductase; EPR, electron paramagnetic resonance; FrdABCD, *E. coli* fumarate reductase; HOQNO, 2-*n*-heptyl-4-hydroxyquinoline-*N*-oxide; Mo-bisMGD, molybdo-bis(molybdopterin guanine dinucleotide) cofactor; MQ, menaquinone; MQH$_2$, menaquinol; NarGHI, *E. coli* nitrate reductase A; NarI(ΔGH), nitrate reductase cytochrome *b* subunit in the absence of the NarGH dimer; STIG, stigmatellin; UQH$_2$, ubiquinol.

that the reduction of the hemes in NarGHI by MQH_2 takes several seconds to complete (*14, 20*). However, it was not possible to follow the initial fast reaction processes occurring during the first few seconds in detail due to the limitations of the spectroscopic techniques employed.

2-*n*-Heptyl-4-hydroxyquinoline-*N*-oxide (HOQNO) is a structural analogue of menaquinol (MQH_2). It has been shown that both HOQNO and stigmatellin (STIG) can inhibit quinol:nitrate oxidoreductase activity (*14*). The binding of HOQNO to NarGHI causes an inversion of the midpoint potentials (E_m) of the two hemes by decreasing the E_m of heme b_H from +120 to +60 mV and increasing the E_m of heme b_L from +25 to +120 mV. The binding of STIG has a moderate effect on heme b_L, increasing its E_m from +25 to +50 mV (*11*). It was reported, in a study using a conventional spectroscopic technique, that the binding of HOQNO and STIG to NarGHI inhibited both the rate and the extent of nitrate-dependent heme reoxidation, but no inhibitory effect was observed on the reduction of the hemes by menadiol (a menaquinol analog) within the time resolution of the spectrophotometers used (*14*). Previously, we have successfully applied the stopped-flow fast kinetic method to investigate the interactions of HOQNO with other terminal reductases in respiratory chains of *E. coli*, dimethyl sulfoxide reductase (DmsABC) (*21*), and fumarate reductase (FrdABCD) (*22*). The stopped-flow technique allows us to study the initial fast reactions that occur immediately after mixing of NarGHI with menaquinol on the previously uncharacterized time scale. Such studies are essential in order to gain insights into the catalytic mechanism of the enzyme.

Electron paramagnetic resonance (EPR) spectroscopy has been used to detect several semiquinone radical species in mutant or wild-type enzymes of *E. coli* respiratory chains, such as FrdABCD (*23*) and quinol oxidases cytochrome *bd* (*24*) and cytochrome *bo₃* (*25*). There is no report on the observation of semiquinone species in wild-type NarGHI. In the mutants of NarGHI, NarGH[C16A]I, and NarGH-[C263A]I, however, a HOQNO-sensitive semiquinone radical species was observed by using EPR (*10*). It is believed that the mutations reduce the rate of the electron transfer in NarGHI, which stabilizes the radical species and makes it possible to be observed. It is of great interest, therefore, to explore the potential of using the fast kinetic method, stopped-flow, to detect the possible formation of the semiquinone radical species in the reduction of the hemes of NarGHI by menaquinol.

In this study, we have utilized the stopped-flow kinetic method to investigate the initial fast reaction processes in the reduction of the hemes in NarGHI by a menaquinol analogue, menadiol, in the absence and in the presence of the inhibitor HOQNO or STIG. We have observed, for the first time, that there are four kinetic phases for the reduction induced by menadiol, and a transient species, likely to be associated with a semiquinone radical anion, is correlated kinetically with one of these kinetic phases. The Q-site inhibitors HOQNO and STIG both inhibit heme reduction, but in kinetically distinct ways. We have also investigated the reduction of the hemes of NarI, that is assembled in the absence of the NarGH subunits (referred to as NarI(ΔGH)). On the basis of these studies, we propose schemes for the mechanism of the reduction of NarGHI by menaquinol and the reoxidation of the reduced enzyme by nitrate.

MATERIALS AND METHODS

Bacterial Strains and Plasmids. *E. coli* LCB2048 [*thi-1, thr-1, leu-6, lacY1, supE44, rpsL175* Δ*nar25*(*narG-narH*) Δ(*nar′U-narZ′*), Ω (Spc^R), Km^R] (*26*) was used for expressing wild-type NarGHI. Wild-type NarGHI and NarI(ΔGH) were expressed from plasmids pVA700 and pCD7, respectively (*8, 10*).

Growth of Cells and Preparation of Membrane Vesicles. LCB2048/pVA700 cells were grown microaerobically in 2-L batches at 30 °C and pH 7.0 in a B. Braun Biostat B fermenter on a growth medium containing 12 g L^{-1} tryptone, 24 g L^{-1} yeast extract, 5 g L^{-1} NaCl, 4 g L^{-1} glycerol, and 0.2 g L^{-1} vitamin B_1. pH was controlled using aliquots of 1 M HCl or 1 M NaOH. The medium also contained 100 μg mL^{-1} streptomycin, 100 μg mL^{-1} ampicillin, and 50 μg mL^{-1} kanamycin. Overexpression of NarGHI was induced with 1 mM isopropyl 1-thio-β-D-galactopyranoside (IPTG) when the culture achieved an OD_{600} of 2.0, after which the culture was grown for a further 10 h. Cells were harvested by centrifugation, and crude membranes were prepared by passage through a French pressure cell and differential centrifugation in a buffer containing 100 mM 3-(*N*-morpholino)-propanesulfonic acid (MOPS) and 5 mM ethylenediamine-tetraacetic acid (EDTA) (pH 7.0) containing the protease inhibitor phenylmethanesulfonyl fluoride (0.2 mM) (*27*). Resuspended crude membranes were layered on top of a 55% (w/v) sucrose layer in an ultracentrifuge tube and subjected to a further centrifugation at 40 000 rpm for 2 h. The floating band containing the cytoplasmic membranes obtained after centrifugation was removed, diluted with buffer, and recentrifuged. Following a further resuspension and centrifugation, the pellet was resuspended, frozen in liquid nitrogen, and then stored at −70 °C until used (*11*). LCB2048 membranes lacking NarGHI were prepared by the same method as above except that ampicillin and IPTG were not used in the growth medium. LCB2048/pCD7 cells (overexpressing NarI(ΔGH)) were grown on Terrific Broth, as previously described (*11*). The cytoplasmic membranes were isolated as described above. Protein concentrations were determined by a modified Lowry assay in the presence of 1% SDS using a BioRad serum albumin protein standard (*28*).

Preparation of Stock Solutions. Menadione (2-methyl-1,4-naphthoquinone) and HOQNO were obtained from Sigma-Aldrich, and STIG was from Fluka Chemie GmbH. Stock solutions of these chemicals were prepared by dissolving them in pure ethanol and were stored at −20 °C in the dark. Menadiol was prepared just before use by reducing menadione with zinc in an acidic ethanol solution as described previously (*29*), placed on ice, and protected from light.

Stopped-flow Experiments and Data Analysis. Stopped-flow experiments were performed using a Sequential Bio SX-17MV stopped-flow spectrofluorimeter (Applied Photophysics Ltd., Leatherhead, U.K.) at either 25 or 5 °C. The flow system was flushed thoroughly with N_2-saturated buffer (100 mM MOPS and 5 mM EDTA, pH 7.0) before experiments. All solutions were saturated with N_2, kept under N_2 atmosphere, and protected from light during experiments. Unless otherwise stated, all concentrations quoted are the initial concentrations before mixing. The mixing ratios of two solutions were all 1:1. In a typical experiment for studying the reduction of the NarGHI hemes by menadiol,

1 mg mL^{-1} of NarGHI (estimated to be 2 μM, based on EPR spin quantitation (*11*)) in 100 mM MOPS and 5 mM EDTA (pH 7.0) was mixed with the menadiol solution in the absence or in the presence of a 60 μM concentration of the inhibitor HOQNO or STIG (preincubated with membranes for 10 min). We found that heme reduction kinetics was relatively independent of menadiol concentration in the range from 350 to 650 μM. Therefore, 500 μM menadiol was chosen for all experiments. For the inhibitors HOQNO and STIG, it has been shown that the maximum inhibition can be achieved at an inhibitor concentration of 60 μM (*14*). Thus, a 60 μM concentration of HOQNO or STIG was used for all inhibition studies.

To investigate the reoxidation of the menadiol-reduced NarGHI hemes by nitrate, a sequential mixing method was adopted. In this method, 1 mg mL^{-1} of NarGHI in 100 mM MOPS and 5 mM EDTA (pH 7.0) was mixed with an equal volume of 500 μM menadiol in the same buffer. After aging for 50 s to allow the complete reduction of the hemes, this mixture was then mixed with an equal volume of 1 mM nitrate in the same buffer, and the reoxidation process was followed.

Since the reduced forms of the hemes in NarGHI have higher absorption at 560 nm compared to the oxidized forms (*14*), the reduction (causing the absorbance to increase) and the oxidation (resulting in the absorbance to decrease) of the hemes can be followed spectroscopically. In both single and sequential mixing experiments, at least three runs were performed, and 500, 2000, or 4000 data points were collected (depending on the time scale used) at two wavelengths, 560 and 575 nm (as reference). The raw data were averaged, and the data for the reduction or reoxidation of the hemes were obtained by subtracting the reference data collected at 575 nm from the data obtained at 560 nm. After subtraction, data were fitted to an appropriate equation using the software supplied by Applied Photophysics. The absorbance changes observed for the reduction of hemes by menadiol (ΔAbs) were fitted to either a double-exponential equation (in the majority of the cases),

$$\Delta\text{Abs} = A_1 e^{-k_1 t} + A_2 e^{-k_2 t} + b \qquad (1)$$

or a single-exponential equation,

$$\Delta\text{Abs} = A e^{-kt} + b \qquad (2)$$

where A_1, A_2, and A are the amplitudes, k_1, k_2, and k are the rate constants, t is time, and b is the end point of the data trace.

The transient species formed in the reduction of the hemes in NarGHI and NarI(ΔGH) by menadiol was observed at 390 nm, where the semiquinone radical anion of menadione has its maximum absorption (*30*, *31*).

RESULTS

Reduction of the Hemes of NarGHI by Menadiol and the Inhibitory Effects of HOQNO and STIG. To investigate the initial fast reaction processes in the reduction of NarGHI by menadiol, the stopped-flow technique was adopted to follow the processes systematically from a short time scale (0.1 s) to a longer time scale (100 s). The inhibitory effects of HOQNO and STIG on the reduction processes were studied
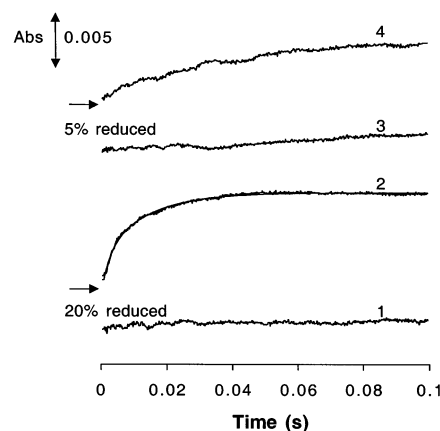

FIGURE 1: Reduction of NarGHI hemes by menadiol and the inhibitory effects of HOQNO and STIG observed on a 0.1-s time scale. Absorbance changes observed after mixing of 1 mg mL^{-1} LCB2048 membranes lacking NarGHI (trace 1) or the membranes enriched with NarGHI (trace 2) in 100 mM MOPS and 5 mM EDTA (pH 7.0) with an equal volume of 500 μM menadiol in the same buffer at 25 °C, in the absence (traces 1 and 2) and in the presence of a 60 μM concentration of the inhibitor HOQNO (trace 3) or STIG (trace 4) by preincubation with the enzyme. The smooth solid line in trace 2 shows the kinetic fit to eq 1, which gives rate constants $k_1 = 412 \pm 40$ s^{-1} and $k_2 = 73 \pm 7$ s^{-1}, and amplitudes $A_1 = -0.0033$ and $A_2 = -0.007$, respectively. The residual of the fit is less than ± 0.0005 (not shown).

by preincubating the membranes with 60 μM concentrations of the inhibitors before mixing with menadiol solutions.

Figure 1 shows the absorbance changes observed on the 0.1-s time scale after mixing of 1 mg mL^{-1} LCB2048 membranes lacking NarGHI (trace 1) or 1 mg mL^{-1} NarGHI-enriched membranes (2 μM, see Material and Methods section) (trace 2) with 500 μM menadiol in 100 mM MOPS and 5 mM EDTA (pH 7.0) at 25 °C in the absence (traces 1 and 2) and in the presence of a 60 μM concentration of the inhibitor HOQNO (trace 3) or STIG (trace 4). As shown by trace 1, there was no detectable reduction after LCB2048 membranes were mixed with the menadiol solution. In contrast to trace 1, after NarGHI-enriched membranes were mixed with the menadiol (trace 2), an increase of the absorbance at 560 nm (after subtracting the absorbance at 575 nm) was observed, indicating that reduction of the hemes occurred. This reduction was fitted to the double-exponential equation (eq 1), as shown by the smooth line, which gave rate constants k_1 and k_2 of 412 ± 40 and 73 ± 7 s^{-1}, respectively. Because of spectral overlap, it should be noted that the reduction observed here is the sum of the reduction contributed by either or both of the hemes in the subunit NarI. In other words, it is not possible to identify which heme receives the electron first just by examining the reduction traces. However, the data obtained from mutants having only one of the two hemes indicate that the electron is received first at the heme b_L since there is no reduction observed for the mutants lacking the heme b_L but there is a reduction observed for the mutants without heme b_H (unpublished data and ref *14*).

In the presence of inhibitors, by comparing trace 3 with trace 4, HOQNO appeared to have a stronger inhibitory effect than STIG on the reduction of NarGHI hemes by menadiol. In the presence of HOQNO (see trace 3), the reduction observed on this time scale appeared to be insignificant, whereas in the presence of STIG, a slow reduction was
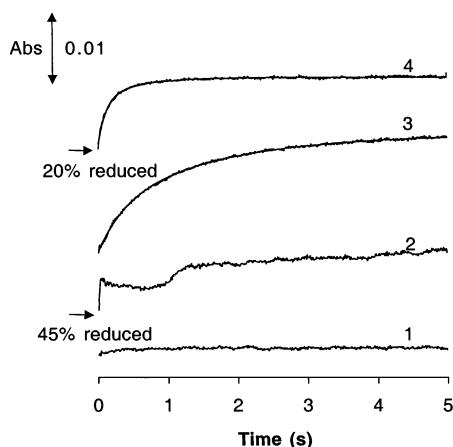
FIGURE 2: Reduction of NarGHI hemes by menadiol and the inhibitory effects of HOQNO and STIG observed on a 5-s time scale. Absorbance changes observed from the same experiments as described in Figure 1 carried out at 25 °C. Traces 1, 2, 3, and 4 represent the data for LCB2048, NarGHI, NarGHI preincubated with HOQNO, and NarGHI preincubated with STIG, respectively. The smooth solid line in trace 3 shows the kinetic fit to eq 1, which gives $k_1 = 3.4 \pm 0.4$ s^{-1}, $k_2 = 0.7 \pm 0.07$ s^{-1}, $A_1 = -0.005$, and $A_2 = -0.012$. The residual of the fit is less than ± 0.0005 (not shown). Similarly, the smooth solid line in trace 4 shows the kinetic fit to eq 1, giving $k_1 = 8.6 \pm 0.09$ s^{-1}, $k_2 = 1.7 \pm 0.2$ s^{-1}, $A_1 = -0.0073$, and $A_2 = -0.0031$. The residual of the fit is less than ± 0.0006 (not shown).

observed (trace 4) which was too slow to yield a reliable kinetic fit on this time scale. In previous studies using conventional spectroscopy, the authors could not detect any effect of HOQNO and STIG on the reduction of the hemes of NarGHI by menadiol (*14, 20*). As shown clearly by traces 3 and 4, HOQNO and STIG both inhibited the reduction of the hemes. Obviously, in the previous studies, the inability to detect the inhibitory effect of the two inhibitors on the reduction was due to the limitation of the time resolution of the spectroscopic technique employed.

It was noted that, in the absence of the inhibitors (trace 2), the reduction of the NarGHI hemes by menadiol was so fast that 20% of the total reduction of the hemes had occurred within the dead time of the stopped-flow instrument (about 2 ms). The total reduction was calculated by subtracting the absorbance value obtained by mixing the enzyme with the buffer from the final value of the reduction trace observed 100 s after the enzyme was mixed with menadiol (see below). Even in the presence of STIG, about 5% of reduction was not observed. To observe the initial missing portion of the reduction, similar experiments were carried out at 5 °C. As expected, a slower reduction compared to that at 25 °C was observed on a 0.1-s time scale after NarGHI-enriched membranes were mixed with menadiol, which could be fitted to eq 1, giving k_1 and k_2 values of 93 ± 9.0 and 0.7 ± 0.07 s^{-1} respectively (data not shown). At this temperature, a small portion of the reduction, about 10%, was still not observed. In the presence of the inhibitors, the reductions observed at 5 °C on this time scale were not significant (data not shown).

Figure 2 shows the absorbance changes observed on a 5-s time scale after mixing of 1 mg mL^{-1} LCB2048 (trace 1) or the NarGHI-enriched membranes (trace 2) in 100 mM MOPS and 5 mM EDTA (pH 7.0) with 500 μM menadiol in the same buffer at 25 °C in the absence (traces 1 and 2) and in the presence of a 60 μM concentration of the inhibitor
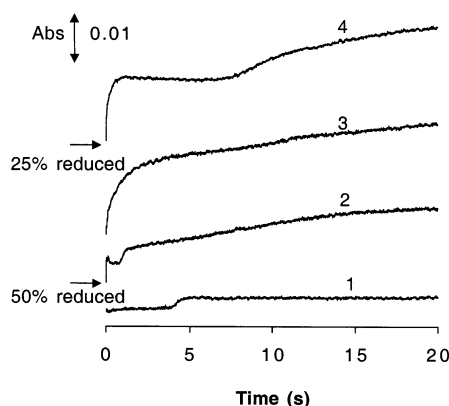

FIGURE 3: Reduction of NarGHI hemes by menadiol and the inhibitory effects of HOQNO and STIG observed on a 20-s time scale. Absorbance changes observed after mixing of 1 mg mL^{-1} of LCB2048 (trace 1) or NarGHI (trace 2) with an equal volume of 500 μM menadiol in 100 mM MOPS and 5 mM EDTA (pH 7.0) at 25 °C, in the absence (traces 1 and 2) and in the presence of a 60 μM concentration of the inhibitor HOQNO (trace 3) or STIG (trace 4) by preincubation.

HOQNO (trace 3) or STIG (trace 4). There was no detectable reduction when LCB2048 membranes were mixed with menadiol, as shown by trace 1. Interestingly, on this extended time scale, after NarGHI-enriched membranes were mixed with the menadiol (trace 2), the change of the absorbance exhibited three phases. After mixing, a very fast increase in absorbance up to about 0.1 s (phase 1), a slower decrease lasting for about 1 s (phase 2), and a relatively fast increase lasting for about 5 s (phase 3) were observed sequentially with time. The appearance of the second phase implied that the reduction of the hemes was followed by a reoxidation (see Discussion section). Since 500 data points were obtained within the 5-s time scale, at the first data point (0.01 s after mixing) about 45% of the reduction, calculated as mentioned earlier, had already occurred. In Figure 2, trace 3 and trace 4 show the observed absorbance changes and the kinetic fits after menadiol solution was mixed with the membranes preincubated with a 60 μM concentration of the inhibitor HOQNO or STIG, respectively. In the presence of HOQNO, the data were fitted to eq 1 (the fitted line was overlapped with the data), which gave $k_1 = 3.4 \pm 0.4$ s^{-1} and $k_2 = 0.7 \pm 0.07$ s^{-1}. STIG had a less inhibitory effect than HOQNO, and the data were fitted to eq 1, with $k_1 = 8.6 \pm 0.09$ s^{-1} and $k_2 = 1.7 \pm 0.2$ s^{-1}. About 20% of the reaction was complete by the time of the first data point.

Experiments similar to those described in Figure 2 were also carried out at 5 °C on a 5 s time scale. It was observed that, in the absence of the inhibitors, the interaction of NarGHI with menadiol exhibited only two phases (compared to Figure 2, trace 2) due to the slower rate of reaction at the decreased temperature (data not shown). In the presence of the inhibitors, the double-exponential fits to eq 1 gave $k_1 = 2.9 \pm 0.3$ s^{-1} and $k_2 = 0.42 \pm 0.04$ s^{-1} for HOQNO, and $k_1 = 6.5 \pm 0.7$ s^{-1} and $k_2 = 1.1 \pm 0.01$ s^{-1} for STIG (data not shown). The effect of temperature on heme reductions was much smaller in the presence of inhibitors. This could be due to some kind of conformational change caused by inhibitor binding.

Figure 3 shows the absorbance changes observed on a 20-s time scale from the same experiments as described in Figure 2 carried out at 25 °C. Traces 1, 2, 3, and 4 represent the
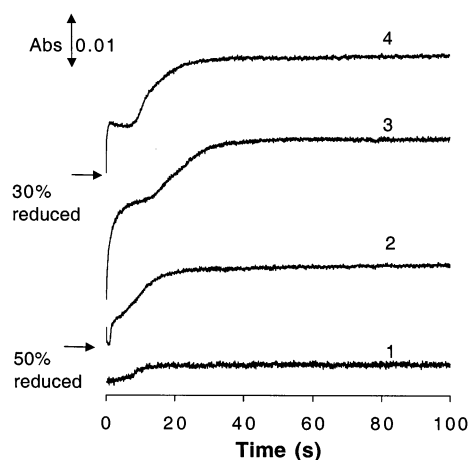
FIGURE 4: Reduction of NarGHI hemes by menadiol and the inhibitory effects of HOQNO and STIG observed on a 100-s time scale. Absorbance changes observed after mixing of 1 mg mL^{-1} of LCB2048 (trace 1) or NarGHI (trace 2) with 500 μM menadiol in 100 mM MOPS and 5 mM EDTA (pH 7.0) at 25 °C in the absence (traces 1 and 2) and in the presence of a 60 μM concentration of the inhibitor HOQNO (trace 3) or STIG (trace 4) by preincubation.

Table 1. Kinetic Constants for the First Phase of Heme Reduction (Phase 1) Observed after Mixing of 1 mg mL^{-1} NarGHI with 500 μM Menadiol in the Absence and in the Presence of 60 μM HOQNO or STIG in 100 mM MOPS and 5 mM EDTA (pH 7.0) at 25 °C

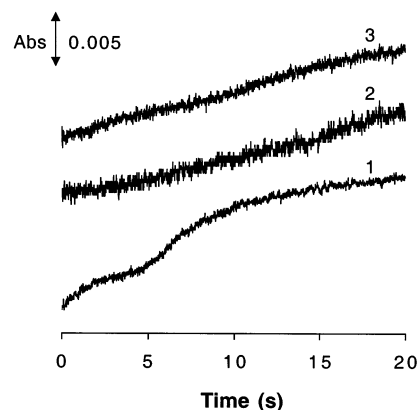|			first reduction of hemes	
sample	time scale (s)	observation	k_2 (s^{-1})	k_2 (s^{-1})
NarGHI	0.1	fast	412 ± 40	73 ± 7.0
NarGHI/HOQNO	0.1	insignificant	na^a	na
NarGHI/STIG	0.1	slow	na	na
NarGHI	5.0	four phases	na	na
NarGHI/HOQNO	5.0	slow	3.4 ± 0.4	0.7 ± 0.07
NarGHI/STIG	5.0	slow	8.6 ± 0.9	1.7 ± 0.2

^{a} na, not applicable.

FIGURE 5: Reduction of NarI(ΔGH) hemes by menadiol and the inhibitory effects of HOQNO and STIG. Absorbance changes observed on a 20-s time scale after mixing of 1 mg mL^{-1} NarI(ΔGH) membranes in 100 mM MOPS and 5 mM EDTA (pH 7.0) with 500 μM menadiol in the same buffer at 5 °C in the absence (traces 1) and in the presence of a 60 μM concentration of the inhibitor HOQNO (trace 2) or STIG (trace 3) by preincubation.

data for LCB2048 membranes, NarGHI-enriched membranes, and NarGHI-enriched membranes preincubated with HOQNO and STIG, respectively. After NarGHI-enriched membranes were mixed with menadiol (trace 2) on this time scale, apart from the three phases observed in Figure 2, another phase appeared (phase 4). In the presence of STIG (trace 4), in addition to the significant inhibition of the reduction, three distinguishable phases of the absorbance change were observed sequentially on this time scale: a fast increase, followed by a slow decrease and then a relatively quick and steady increase. In the presence of HOQNO, the observed trace did not clearly exhibit multiple phases (trace 3). When experiments similar to those described in Figure 3 were carried out at 5 °C on a 20-s time scale, multiple phases similar to that described in Figure 2 (trace 2) were observed for the interaction of NarGHI-enriched membranes with menadiol, but phase 3 appeared later, about 5 s after mixing rather than 1 s (data not shown).

Figure 4 shows the absorbance changes observed on a 100-s time scale from the same experiments carried out at 25 °C as described in Figure 3. Traces 1, 2, 3, and 4 represent the data for LCB2048, NarGHI-enriched membranes, preincubated with HOQNO, and with STIG, respectively. For the interaction of NarGHI with menadiol (trace 2), phase 4 of the reduction trace (see the description of Figure 3 above) increased with time and reached a plateau about 20 s after mixing. In the presence of HOQNO (trace 3), only two reduction phases were observed, and the plateau of the trace appeared much later, about 30 s after mixing. On this time scale in the presence of STIG (trace 4), three distinguishable phases were clearly observed, especially the decrease of absorbance that followed the first reduction phase. Kinetic constants for the first phase of heme reduction (phase 1), observed within 0.1 and 5 s after mixing of 1 mg mL^{-1} NarGHI with 500 μM menadiol in the absence and in the presence of a 60 μM concentration of HOQNO or STIG at 25 °C, are summarized in Table 1.

Reduction of the Hemes of NarI(ΔGH) by Menadiol and the Inhibitory Effects of HOQNO and STIG. To investigate the role of the prosthetic group composition of the membrane-extrinsic catalytic dimer (NarGH), studies of the interaction of menadiol with NarI(ΔGH) were performed. It was observed that the rate for the reduction of the hemes was significantly decreased compared to that of the holoenzyme. No significant reduction was observed within 0.1 s after mixing of 1 mg mL^{-1} NarI(ΔGH)-enriched membranes in 100 mM MOPS and 5 mM EDTA (pH 7.0) with 500 μM menadiol at 5 °C, and even on the 5-s time scale, only a slow reduction appeared (data not shown). On the 20-s time scale, as shown in Figure 5, a clear two-phase reduction was observed: the first phase lasted for about 5 s, and then the second phase appeared (trace 1). Both phases could be fitted to the single-exponential equation (eq 2) separately to give the same rate constant of 0.2 ± 0.02 s^{-1}. After preincubation with a 60 μM concentration of inhibitor HOQNO (trace 2) or STIG (trace 3), the reduction rate was reduced, and the two-phase feature was not observed on this time scale.

The absorbance changes observed on the 100-s time scale are shown in Figure 6. For the interaction of menadiol with NarI(ΔGH) (trace 1), the reduction trace approached a plateau about 30 s after mixing. The effect of the inhibitors on the reduction kinetics was obvious. In the presence of HOQNO (trace 2), there was no clear-cut two-phase feature (compared to trace 1). In the presence of STIG (trace 3), however, the two-phase feature was observed, but the second
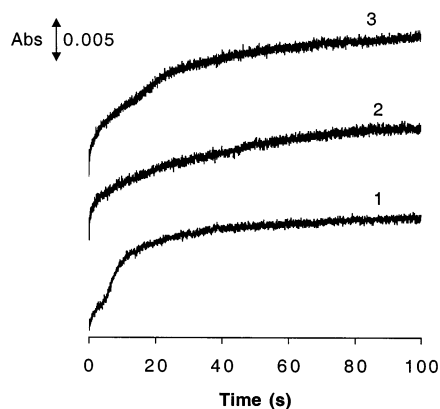
FIGURE 6: Absorbance changes observed on a 100-s time scale from the same experiments as described in Figure 5. Traces 1, 2, and 3 represent the reaction of menadiol with NarI(ΔGH), NarI(ΔGH) preincubated with HOQNO, and NarI(ΔGH) preincubated with STIG, respectively.
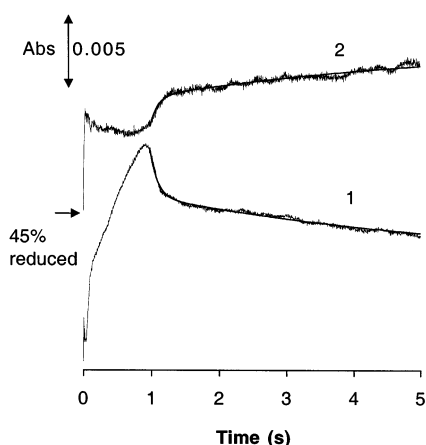

FIGURE 7: Observation of the transient species and its correlation with heme reduction in NarGHI by menadiol. Absorbance changes observed after mixing of 1 mg mL^{-1} of NarGHI membranes with 500 μM menadiol in 100 mM MOPS and 5 mM EDTA (pH 7.0) at 25 °C. Trace 1 represents the observed formation and decay of the transient species at 390 nm, and the smooth solid line in trace 1 shows the kinetic fit to eq 1, giving rate constants $k_1 = 9.24 \pm 0.9$ s^{-1} and $k_2 = 0.22 \pm 0.02$ s^{-1}, and amplitudes $A_1 = 0.0042$ and $A_2 = 0.005$. The residual of the fit is less than ± 0.0006 (not shown). Trace 2 shows the observed reduction of the hemes at 560 nm (after subtracting the 575 nm absorbance), and the smooth solid line shows the kinetic fit to eq 1, with $k_1 = 9.23 \pm 0.9$ s^{-1}, $k_2 = 0.22 \pm 0.02$ s^{-1}, $A_1 = -0.0024$, and $A_2 = -0.0041$. The residual of the fit is less than ± 0.0004 (not shown).

phase appeared much later (about 15 s after mixing) than in the absence of the inhibitor.

Transient Species Formed in the Reduction of the Hemes of NarGHI and NarI(ΔGH) by Menadiol. It has previously been reported that a mutation in NarGHI stabilized a semiquinone radical species by reducing the rate of electron transfer in NarGHI, which resulted in the observation of the radical species using EPR (*10*). The menadione radical anion has an absorption maximum at 390 nm (*30, 31*). In this study, therefore, we utilized the stopped-flow fast kinetic method to detect the formation of the radical species spectroscopically. Figure 7 shows the absorbance changes observed at 390 (trace 1) and 560 nm (after subtracting the 575 nm absorbance) (trace 2) after mixing of 1 mg mL^{-1} NarGHI-enriched membranes with 500 μM menadiol in 100 mM MOPS and 5 mM EDTA (pH 7.0) at 25 °C. In Figure 7,
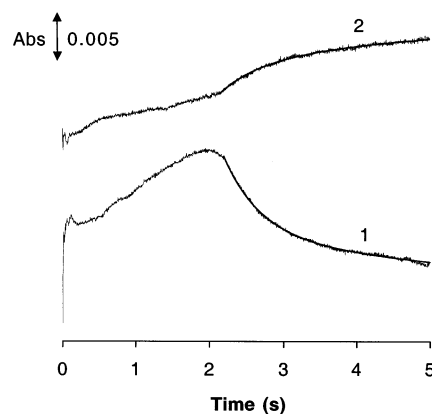

FIGURE 8: Observation of the transient species and its correlation with heme reduction in NarI(ΔGH) by menadiol. Absorbance changes observed after mixing of 1 mg mL^{-1} NarI(ΔGH) membranes with 500 μM menadiol in 100 mM MOPS and 5 mM EDTA (pH 7.0) at 25 °C. Trace 1 represents the observed formation and decay of the transient species at 390 nm, and the smooth solid line in trace 1 shows the kinetic fit to eq 1, which gives $k_1 = 2.3 \pm 0.23$ s^{-1}, $k_2 = 0.33 \pm 0.03$ s^{-1}, $A_1 = 0.0087$, and $A_2 = 0.0071$. The residual of the fit is less than ± 0.0005 (not shown). Trace 2 shows the observed reduction of the hemes at 560 nm (after subtracting the 575 nm absorbance), and the smooth solid line in trace 2 shows the kinetic fit to eq 1, giving $k_1 = 2.1 \pm 0.21$ s^{-1}, $k_2 = 0.39 \pm 0.04$ s^{-1}, $A_1 = -0.0031$, and $A_2 = -0.0053$. The residual of the fit is less than ± 0.0004 (not shown).

trace 1 clearly demonstrates the kinetic profile of the formation and decay of a transient species, and trace 2 represents the reduction kinetics of the NarGHI hemes with three phases. Interestingly, the decay of this transient species was kinetically correlated to the buildup of the second reduction of the hemes (phase 3), and they both were best fitted to the double-exponential equation (eq 1), giving similar rate constants, $k_1 = 9.24 \pm 0.9$ s^{-1} and $k_2 = 0.22 \pm 0.02$ s^{-1} for the decay of the transient species, and $k_1 = 9.23 \pm 0.9$ s^{-1} and $k_2 = 0.22 \pm 0.02$ s^{-1} for the buildup of the second reduction.

In the reduction of the hemes of NarGHI preincubated with HOQNO or STIG, the transient species was formed and decayed with slower rates compared with the situation in the absence of inhibitors (data not shown). This transient species was also kinetically correlated to the second reduction of the hemes. The decay of the transient species and the buildup of the second reduction of the hemes were both fitted to eq 1, yielding similar rate constants. In the presence of HOQNO, the rate constants were $k_1 = 0.13 \pm 0.01$ s^{-1} and $k_2 = 0.01 \pm 0.001$ s^{-1} for the decay of the transient species, and $k_1 = 0.12 \pm 0.01$ s^{-1} and $k_2 = 0.01 \pm 0.001$ s^{-1} for the buildup of the second reduction of the hemes. In the presence of STIG, $k_1 = 2.42 \pm 0.24$ s^{-1} and $k_2 = 0.09 \pm 0.01$ s^{-1} for the decay of the transient species, and $k_1 = 2.18 \pm 0.22$ s^{-1} and $k_2 = 0.09 \pm 0.01$ s^{-1} for the buildup of the second reduction.

For NarI(ΔGH), the transient species was also observed. Figure 8 shows the absorbance changes observed at 390 (trace 1) and 560 nm (after the subtraction of 575 nm absorbance) (trace 2) after mixing of 1 mg mL^{-1} NarI(ΔGH)-enriched membranes with 500 μM menadiol in 100 mM MOPS and 5 mM EDTA (pH 7.0) at 25 °C. This transient species was also kinetically correlated to the reduction of the hemes. However, its formation and decay were much slower than those for the holoenzyme (Figure 7). Table 2

Table 2. Comparison of Kinetic Constants for the Decay of the Transient Species and for the Second Reduction of the Hemes Observed after Mixing of 1 mg mL^{-1} NarGHI or NarI(ΔGH) with 500 μM Menadiol in 100 mM MOPS and 5 mM EDTA (pH 7.0) at 25 °C

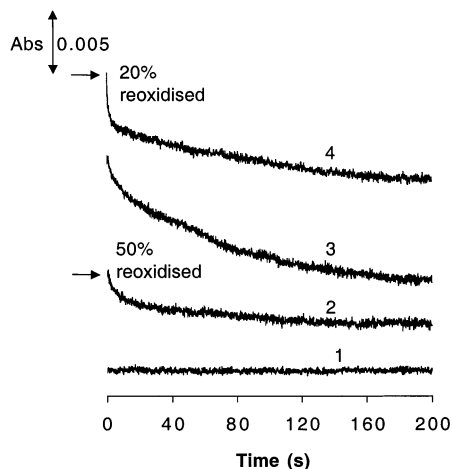|	decay of transient species		second reduction of hemes	
sample	k_1 (s^{-1})	k_2 (s^{-1})	k_1 (s^{-1})	k_2 (s^{-1})
NarGHI	9.24 ± 0.9	0.22 ± 0.02	9.23 ± 0.9	0.22 ± 0.02
NarGHI/ HOQNO	0.13 ± 0.01	0.01 ± 0.001	0.12 ± 0.01	0.01 ± 0.001
NarGHI/STIG	2.42 ± 0.24	0.09 ± 0.01	2.18 ± 0.22	0.09 ± 0.01
NarI(ΔGH)	2.30 ± 0.23	0.33 ± 0.03	2.10 ± 0.21	0.39 ± 0.04

FIGURE 9: Reoxidation of menadiol-reduced NarGHI hemes by nitrate and the inhibitory effects of HOQNO and STIG. Absorbance changes observed by mixing 1 mg mL^{-1} LCB2048 membranes (trace 1) or NarGHI membranes (trace 2) with 500 μM menadiol in 100 mM MOPS and 5 mM EDTA (pH 7.0) at 25 °C in the absence (traces 1 and 2) and in the presence of a 60 μM concentration of the inhibitor HOQNO (trace 3) or STIG (trace 4) by preincubation with the enzyme, and then by mixing the mixture with 1 mM nitrate in the same buffer.

summarizes the rate constants for the decay of the transient species and the buildup of the second reduction of the hemes in NarGHI and NarI(ΔGH).

Reoxidation of Menadiol-Reduced NarGHI Hemes by Nitrate and the Inhibitory Effects of HOQNO and STIG. A sequential stopped-flow method was adopted to investigate electron transfer from NarI through the [Fe-S] clusters of NarH to the Mo-bisMGD located in NarG. In these experiments, 1 mg mL^{-1} membranes was mixed rapidly with 500 μM menadiol in 100 mM MOPS and 5 mM EDTA (pH 7.0) at 25 °C, resulting in the reduction of the hemes. After aging for 50 s, this mixture was then mixed with 1 mM nitrate solution in the same buffer. Using this method, the reoxidation of the hemes of NarGHI induced by the reduction of the nitrate can be followed spectroscopically. As a control, the same sequential stopped-flow experiment was also carried out for LCB2048 membranes. In this case, as shown in Figure 9, trace 1, there was no significant absorbance change after mixing with the nitrate solution, indicating that there was no reoxidation in the system. For NarGHI (trace 2), a decrease of absorbance was observed, indicating a reoxidation of the hemes. It was noticed that, when the first data point was taken (0.1 s after mixing), about 50% of the hemes were already reoxidised as a consequence of nitrate reduction.

When the NarGHI was reduced after preincubation with HOQNO or STIG, the reoxidation process was affected significantly, and two inhibitors exhibited different inhibitory kinetics. HOQNO (trace 3) had a stronger effect than STIG (trace 4) on the reoxidation process.

DISCUSSION

In the work reported herein, we have observed that the reduction of NarGHI hemes by menadiol proceeds via four kinetic phases (phases 1−4). These phases are as follows: (1) rapid first reduction, (2) slow reoxidation, (3) moderately fast second reduction, and (4) slow reduction to the fully reduced form. Both inhibitors HOQNO and STIG have strong effects on the reduction and reoxidation kinetics. As menadiol is an analogue of MQH$_2$, the data we reported here could represent the situation for NarGHI heme reduction by MQH$_2$ and the reoxidation by nitrate. On the basis of the results, we propose mechanisms for the reduction of NarGHI by MQH$_2$ (Scheme 1) and the reoxidation of reduced NarGHI by nitrate (Scheme 2).

In Scheme 1, we propose that, after mixing, MQH$_2$ rapidly binds to NarGHI to form a complex (step 1). In this complex, initially the hemes b_L and b_H, the iron−sulfur clusters, and the Mo-bisMGD cofactor are all in their oxidized forms. Upon formation of the complex, MQH$_2$ immediately delivers one electron (the first electron) to heme b_L, accompanied by a fast deprotonation, releasing one proton to the periplasmic side of the membrane (step 2). This reaction is observed as the first reduction phase of the hemes (phase 1, Figures 1−3 and 7) and results in the formation of a complex of the hydroquinone radical (MQH$^\bullet$) bound to NarGHI. In this complex, heme b_L is in its reduced form, while heme b_H, the iron−sulfur clusters, and Mo-bisMGD cofactor are still in their oxidized forms. The electron is next transferred from the reduced heme b_L to the oxidized heme b_H (intra-subunit electron transfer, step 3). Heme b_H, reduced in step 3, transfers the electron to the iron−sulfur clusters (inter-subunit electron transfer, step 4, phase 2). The inter-subunit electron transfer from the subunit NarI (via heme b_H) to the subunit NarH (through [3Fe-4S] clusters) would be slower compared with intra-subunit electron transfer from heme b_L to heme b_H. This is because the difference between the E_m values of heme b_H and the [3Fe-4S] cluster (60 mV) is lower than that between the two hemes (100 mV), although both gradients of E_m are in the direction favorable for electron transfer. Thus, during step 4, heme b_H would be only partially oxidized (strictly speaking, the electron density on heme b_H could be decreased during this step). This is in agreement with the observation that the absorbance is decreased but not to the background level during the reoxidation phase, described as phase 2 in Figures 2, 3, and 7. Step 4 leads to partial reduction of the Fe−S−Mo box. That phase 2 arises from electron transfer from heme b_H to the prosthetic groups of the catalytic dimer is evident from the absence of a similar phase in membranes lacking NarGH (NarI(ΔGH)) (Figures 5 and 6). In parallel to the reoxidation, a deprotonation also takes place and releases a second proton into the periplasm, which gives a complex of menasemiquinone radical anion (MQ$^{\bullet-}$) bound to the enzyme. The MQ$^{\bullet-}$ delivers the second electron to the oxidized heme b_L (step 5, phase 3) followed by an intra-subunit electron transfer from heme b_L to heme b_H (step 6) and an inter-subunit electron transfer from heme

Scheme 1. Simplified Mechanism for the Reduction of NarGHI by Menadiol[a]
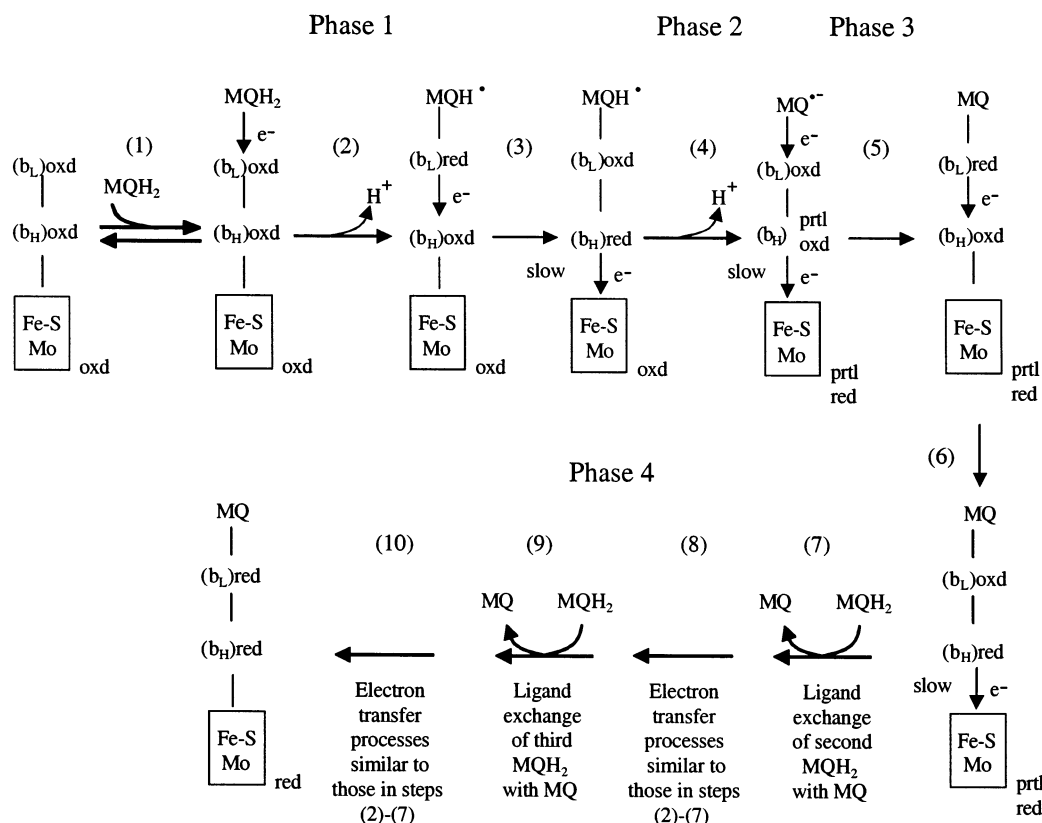
[a] For simplicity, the following has been done. (i) The iron-sulfur clusters and the Mo-bisMGD cofactor are symbolized by a box. The subscripts "oxd", "red", "prtl oxd", and "prtl red" represent the oxidized, reduced, partially oxidized, and partially reduced forms, respectively. (ii) Only the association of the first MQH_2 to the enzyme and the subsequent electron-transfer processes are shown. After step 6, the association of the second MQH_2 by a ligand-exchange reaction replacing MQ from the binding site is simplified by step 7, and the subsequent electron-transfer processes (similar to those in steps 2−7) are simplified by an arrow (step 8). The same simplifications are also made for the association of the third MQH_2 (step 9) and the subsequent electron-transfer processes (step 10) leading to the final product. (iii) The inter-subunit electron transfer from heme b_H to iron-sulfur clusters would be slower compared with intra-subunit electron transfer from heme b_L to heme b_H (see the text), and this process is labeled "slow". Heme b_H would take two steps (4 and 5) to be fully oxidized.

Scheme 2. Simplified Mechanism for the Reoxidation of Menadiol-Reduced NarGHI by Nitrate[a]
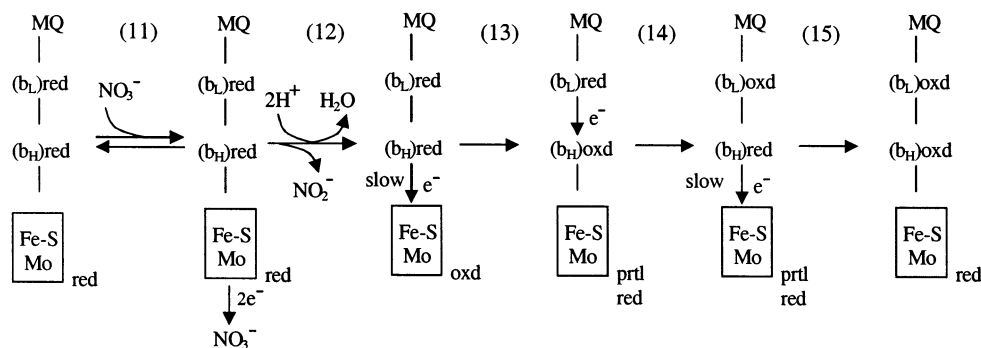
[a] For simplicity, the iron-sulfur clusters and the Mo-bisMGD cofactor are symbolized by a box and the subscripts are as in Scheme 1. For the same reason as described for Scheme 1, the inter-subunit electron-transfer processes from heme b_H to iron−sulfur clusters are labeled "slow". For simplicity, however, heme b_H is described to be fully oxidized in a slow single step (step 13 or 15), which would be equivalent to the two steps in Scheme 1 (steps 4 and 5) in terms of time scale.

b_H to the iron−sulfur cluster, accompanied by a ligand-exchange reaction replacing MQ by MQH_2 (step 7).

Mo(VI) can be reduced to Mo(IV) by receiving two electrons. We assume that only those two iron−sulfur clusters which have positive E_m are involved in electron transfer (the other two clusters have negative E_m). The two clusters and two hemes each can be reduced by accepting one electron. Together, it would take six electrons from three menadiol molecules for a NarGHI molecule to be fully reduced since

menaquinol is a two-electron donor (if one or two more iron−sulfur clusters are involved in electron transfer, more MQH_2 would be required). Eventually, in the absence of nitrate, the hemes, the iron−sulfur clusters which are involved in electron transfer, and the Mo-bisMGD cofactor are all reduced, and this would lead to a scheme with about 20 steps. To simplify the scheme, only the association of the first MQH_2 to the enzyme and the subsequent electron-transfer processes are shown. After step 6, the association

of the second MQH$_2$ by a ligand-exchange reaction replacing MQ from the binding site is simplified by step 7, and the subsequent electron-transfer processes (similar to those in steps 2−7) are simplified by an arrow (step 8). The same simplifications are also made for the association of the third MQH$_2$ (step 9) and the subsequent electron-transfer processes (step 10) leading to the final product, the complex of MQ with the fully reduced enzyme. It should be pointed out that there could be an equilibrium between MQ or MQH$_2$ (if it is available) with the fully reduced enzyme.

Steps 1 and 2 are rapid and result in a fast reduction phase of the hemes (phase 1), which can be fitted to the double-exponential equation (eq 1) to give k_1 and k_2 values of 412 ± 40 and 73 ± 7 s^{-1}, respectively. The dependence of both observed k_1 (the fast phase) and k_2 (the slow phase) values on menadiol concentration ([MQH$_2$]) exhibited a hyperbolic curve when the concentration of menadiol was increased from 50 to 700 μM (before 1:1 mixing) (data not shown), which can be described by a two-step equilibrium model (34): a fast equilibrium of menadiol (MQH$_2$) binding to the oxidized enzyme (Enzyme$_{oxd}$), followed by a slow electron-transfer process (rate limiting) from the bound menadiol to the oxidized enzyme (heme b_L). This yields a complex of hydroquinone radical (MQH$^•$) with partially reduced enzyme (Enzyme$_{prtlred}$), accompanied by a deprotonation (see Scheme 1),

$$MQH_2 + Enzyme_{oxd} \leftrightarrow (MQH_2-Enzyme_{oxd}) \leftrightarrow$$
$$(MQH^•-Enzyme_{prtl\,red}) + H^+$$
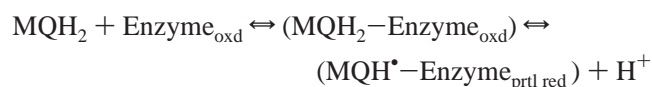
The observed rate constants k_1 and k_2 can be fitted to the equation $k_{obs} = k_{2nd\,fwd}[MQH_2]/(K_{d\,first} + [MQH_2]) + k_{2nd\,rvs}$, where $K_{d\,1st}$ is the apparent dissociation constant of the first equilibrium, and $k_{2nd\,fwd}$ and $k_{2nd\,rvs}$ are the rate constants for the forward and the reverse reactions of the second equilibrium, respectively (34).

The fit of the observed k_1 (for the fast phase) to the equation gave $K_{d\,1st} = 65 ± 10$ μM and $k_{2nd\,fwd} = 450 ± 50$ s^{-1}, the fit of k_2 (for the slow phase) yielded $K_{d\,1st} = 180 ± 20$ μM and $k_{2nd\,fwd} = 110 ± 10$ s^{-1}, and both fits gave an approximate zero value for $k_{2nd\,rvs}$ (data not shown). Obtaining two different $K_{d\,1st}$ values may imply the presence of two menadiol binding sites in the enzyme, one with higher affinity for menadiol (65 μM) than the other (180 μM). This is in agreement with the inhibition data, which indicate that there could be more than one menaquinol binding site in NarGHI. The rate constant for the forward reaction of the second equilibrium, $k_{2nd\,fwd}$, can be described as an apparent rate constant for the electron transfer from bound menadiol to heme b_L of the oxidized enzyme. The 4-fold greater $k_{2nd\,fwd}$ for the observed fast phase compared to the one for the slow phase could indicate that this high-affinity binding site is closer to heme b_L than the low-affinity site. The rate constant for the reverse reaction of the second equilibrium, $k_{2nd\,rvs}$, is approximately zero for both the fast and slow phases, indicating that the reverse electron transfer from reduced heme b_L back to oxidized menadiol is not feasible due to the gradients of the reduction potentials between the reduced heme b_L and the oxidized heme b_H, and between the heme b_L and the oxidized menadiol, which are favorable for an electron transfer from the reduced heme b_L to the oxidized heme b_H, rather than back to the oxidized menadiol. It is

likely, therefore, that the observed rate constants of the first phase of heme reduction, k_1 and k_2, represent binding of menadiol at a high- and a low-affinity site and the subsequent electron transfer from the site to heme b_L, respectively.

After preincubation of NarGHI with the inhibitor HOQNO or STIG, the rate for reduction of NarGHI hemes by menadiol was significantly reduced (Figures 1−4). Furthermore, these two inhibitors exhibit different behaviors. First, HOQNO appears to be a stronger inhibitor of heme reduction than STIG. Second, three phases were clearly observed on the 100-s time scale in the presence of STIG, and only two phases were observed in the presence of HOQNO (Figure 4). The loss of the reoxidation phase (phase 2) when HOQNO is bound to NarGHI could be due to significant slowing-down of the electron-transfer process from heme b_L to heme b_H (step 3). This can be understood from the effects of inhibitor binding on the midpoint potentials (E_m) of the two hemes. Binding of HOQNO to NarGHI causes a reversal of the E_m values of the two hemes (11), which results in a change of the E_m differences between the two hemes from 100 mV in the direction favorable to the electron transfer from the heme b_L to heme b_H to 60 mV in the direction against the electron transfer. Binding of STIG results in an increase of the E_m of heme b_L (11), which leads to a decrease of the E_m differences between the two hemes from 100 to 70 mV, but still in the direction favorable to the electron transfer. Thus, the inhibitory effect of STIG is smaller than that of HOQNO. It has been reported in a previous steady-state kinetic study that STIG exhibited stronger inhibition than HOQNO on the activity of NarGHI (14). However, it is not valid to make a direct comparison between the different inhibitory effects observed in this transient kinetic study and that from the steady-state kinetic one, because the reaction systems under investigations are different. In this transient kinetic study, we investigate the effect of inhibitors on heme reduction in NarGHI in the absence of the substrate (nitrate), whereas in the steady-state kinetic study, the authors measured the effect of inhibitors on the activity of the enzyme in the presence of the substrate (nitrate).

The inhibition by the MQH$_2$ analogue, HOQNO, on the reduction of NarGHI hemes by menadiol implies that there may be more than one MQH$_2$ binding site (Q-site) in NarGHI. If only one Q-site exists in NarGHI, then the reduction of the NarGHI preincubated with HOQNO can take place only after a ligand exchange replacing HOQNO with MQH$_2$ in the binding site. This ligand-exchange reaction, as expected, would delay the formation of the complex of menadiol with NarGHI (step 1). After formation of the complex, however, the reduction would proceed with kinetics similar to the pattern in the absence of HOQNO. The loss of the reoxidation phases by HOQNO binding suggests that HOQNO is still bound to the enzyme during the reduction processes induced by menadiol.

On the basis of steady-state kinetic analyses (19), it has been suggested that NarGHI contains multiple Q-sites, one specific for MQH$_2$ and another for UQH$_2$. This is consistent with results suggesting that both quinol species can support NarGHI-mediated respiratory growth on nitrate (32, 33). We have demonstrated by fluorescence quench titration that there appears to be only a single dissociable site that is able to bind the MQH$_2$ analogue HOQNO (11, 20). However, we cannot rule out the possibility of existence of another binding

site for a different quinol. It should be emphasized that the chemical structures of HOQNO and MQH_2 molecules are different, although they are analogues; specifically, there are a nitrogen and a relatively long aliphatic side chain in HONQO. These structural differences may result in HOQNO and MQH_2 preferring to bind to different residues. In other words, they might prefer to bind at different sites, as suggested for MQH_2 and UQH_2 (*19*). This would explain the result of fluorescence quench titration that there is only one HOQNO binding site in NarGHI.

The reduction of NarI(ΔGH) hemes by menadiol exhibits two kinetic phases (Figure 5); compared to NarGHI (Figures 2–4), the reoxidation phase of the hemes (Phase 2) is not observed. This is consistent with the suggestion that this phase is due to the inter-subunit electron transfer from NarI to the prosthetic groups of the membrane-extrinsic NarGH dimer. There is no NarGH dimer in NarI(ΔGH).

According to Scheme 1, following the partial reoxidation of the hemes and a deprotonation of the hydroquinol radical (step 4, phase 2), a transient species of a complex of menadione radical anion with the enzyme is formed. Moreover, the decay of this transient species can be correlated kinetically to the second reduction of hemes (step 5, phase 3). It has been reported that menadione radical anion has an absorption maximum at 390 nm (*30, 31*), with a molar extinction coefficient of 13 000 M^{-1} cm^{-1} (*30*). The transient species observed at 390 nm in this study has a molar extinction coefficient about 14 000 M^{-1} cm^{-1}, calculated using the absorbance value ($\sim$0.014) and the concentration of the membrane protein (1 μM after mixing). In this calculation, it is assumed that there would be only one menadiol binding site in each NarGHI molecule (although the possibility of more than one binding site cannot be ruled out), and all binding sites would be fully occupied by menadiol since the concentration of menadiol is in excess. The value of the molar extinction coefficient calculated here is close, but not equal, to the one published for menadione radical anion. This is understandable because the published molar extinction coefficient is for free menadione radical anions and the one calculated by us is for a transient species associated with a membrane protein. We propose, therefore, that the transient species observed at 390 nm is a complex of menadione radical anion with the partially reduced NarGHI. The observation of this transient species (Figure 7) and its kinetic correlation to heme reduction (Table 2) strongly support the mechanism for the reduction of NarGHI by MQH_2 proposed in Scheme 1. To further characterize this transient species, EPR studies of menadiol-reduced nitrate reductase and the reoxidation of dithionite-reduced enzyme by nitrate are in progress in our laboratory.

In the presence of HOQNO or STIG, the decay rate of the transient species was significantly reduced (Table 2), indicating that the presence of the inhibitor stabilized the transient species. This can be explained from the effects of HOQNO and STIG binding on the midpoint potentials of the two hemes (E_m). As discussed earlier, the change of the E_m gradient induced by inhibitor binding reduces the rate of electron transfer from the heme b_L to heme b_H (step 3), which in turn slows-down the electron transfer from $MQ^{\bullet-}$ to heme b_L (step 5) and thus stabilizes the transient species. The transient species formed in the presence of the inhibitor has components similar to those described earlier: a complex

of $MQ^{\bullet-}$ with the partially reduced NarGHI but bound with the inhibitor in this case.

In NarI(ΔGH), the E_m differences between the two hemes (*11*) was in the direction against the electron transfer from the heme b_L to heme b_H (step 3). Therefore, the formation and the decay of the transient species were significantly slowed (Figure 8 and Table 2). The transient species, in this case, would be a complex of $MQ^{\bullet-}$ associated with the partially reduced NarI(ΔGH).

Scheme 2 is proposed as a simplified mechanism for the reoxidation of menaquinol-reduced NarGHI by nitrate. Like Scheme 1, it is assumed in Scheme 2, for simplicity, that MQ would bind to the reduced enzyme through all reaction processes. In Scheme 2, after mixing with the solution containing menadiol-reduced NarGHI, nitrate binds to the reduced NarGHI via an equilibrium (step 11), to form a complex. Upon the formation of the complex, the reduced NarGHI reduces the nitrate to nitrite by two-electron reduction and takes two protons from the cytoplasmic side of the membrane (step 12). This is followed by release of nitrite and a water molecule from the complex. The reduction of nitrate by the enzyme results in the oxidation of the Mo-bisMGD cofactor, which initiates a series of electron-transfer processes, occurring sequentially from the reduced iron–sulfur clusters to the oxidized Mo-bisMGD cofactor, from the reduced heme b_H to the reoxidized iron–sulfur cluster (resulting in the reoxidation of heme b_H (step 13)), from the reduced heme b_L to the reoxidized heme b_H (step 14), and from the reduced heme b_H to the reoxidized iron–sulfur clusters and to the oxidized Mo-bisMGD cofactor (step 15); eventually, both hemes are reoxidized. For the same reason as described for Scheme 1, the inter-subunit electron-transfer processes are labeled "slow". For simplicity, however, heme b_H is described to be fully oxidized in a slow single step (step 13 or 15), which would be equivalent to the two steps in Scheme 1 (steps 4 and 5) in terms of time scale.

When the NarGHI hemes were reduced after preincubation of NarGHI with HOQNO or STIG, the rate of the reoxidation of this reduced enzyme by nitrate was decreased (Figure 9). This could be again due to the change of the E_m gradient between the two hemes induced by inhibitor binding, which would lead to the decrease of the rate for the electron transfer from the heme b_L to heme b_H (step 14). Furthermore, these results agree with our speculation that HOQNO and MQH_2 could bind at different sites in NarGHI.

In summary, this is the first report on the transient kinetic study for the reduction of NarGHI hemes by menaquinol. We found that the reduction exhibits four phases, and a transient species, described as a complex of $MQ^{\bullet-}$ associated with the enzyme, is kinetically correlated to the second reduction of the hemes. The inhibitory effect of HOQNO on the reduction indicates that there are more than one menaquinol binding sites in NarGHI. The schemes proposed in this study can help us to understand the mechanism of electron transfer in the reduction of NarGHI by menaquinol and in the reoxidation of the reduced NarGHI by nitrate.

REFERENCES

1. Gennis, R. B., and Ferguson-Miller, S. (1996) *Curr. Biol. 6*, 36–38.

2. Jones, R. W., Lamont, A., and Garland, P. B. (1980) *Biochem. J. 190*, 79–94.

3. Blasco, F., Iobbi, C., Giordano, G., Chippaux, M., and Bonnefoy, V. (1989) *Mol. Gen. Genet. 218*, 249–256.

4. Richardson, D. J., and Watmough, N. J. (1999) *Curr. Opin. Chem. Biol. 3*, 207–219.

5. Rothery, R. A., Magalon, A., Giordano, G., Guigliarelli, B., Blasco, F., and Weiner, J. H. (1998) *J. Biol. Chem. 273*, 7462–7469.

6. Magalon, A., Asso, M., Guigliarelli, B., Rothery, R. A., Bertrand, P., Giordano, G., and Blasco, F. (1998) *Biochemistry 37*, 7363–7370.

7. Augier, V., Asso, M., Guigliarelli, B., More, C., Bertrand, P., Santini, C. L., Blasco, F., Chippaux, M., and Giordano, G. (1993) *Biochemistry 32*, 5099–5108.

8. Guigliarelli, B., Magalon, A., Asso, M., Bertrand, P., Frixon, C., Giordano, G., and Blasco, F. (1996) *Biochemistry 35*, 4828–4836.

9. Hacket, N. R., and Bragg, P. D. (1982) *FEMS Microbiol. Lett. 13*, 213–217.

10. Magalon, A., Rothery, R. A., Giordano, G., Blasco, F., and Weiner, J. H. (1997) *J. Bacteriol. 179*, 5037–5045.

11. Rothery, R. A., Blasco, F., Magalon, A., Asso, M., and Weiner, J. H. (1999) *Biochemistry 38*, 12747–12757.

12. Blasco, F., Guigliarelli, B., Magalon, A., Asso, M., Giordano, G., and Rothery, R. A. (2001) *Cell. Mol. Life Sci. 58*, 179–193.

13. Rothery, R. A., Blasco, F., Magalon, A., and Weiner, J. H. (2001) *J. Mol. Microbiol. Biotechnol. 3*, 273–283.

14. Magalon, A., Rothery, R. A., Lemesle-Meunier, D., Frixon, C., Weiner, J. H., and Blasco, F. (1998) *J. Biol. Chem. 273*, 10851–10856.

15. Dias, J. M., Than, M. E., Humm, A., Huber, R., Bourenkov, G. P., Bartunik, H. D., Bursakov, S., Calvete, J., Caldeira, J., Carneiro, C., Moura, J. J., Moura, I., and Romao, M. J. (1999) *Struct. Fold Des. 7*, 65–79.

16. Breton, J., Berks, B. C., Reilly, A., Thomson, A. J., Ferguson, S. J., and Richardson, D. J. (1994) *FEBS Lett. 345*, 76–80.

17. Jormakka, M., Tornroth, S., Byrne, B., and Iwata, S. (2002) *Science 295*, 1863–1868.

18. Morpeth, F. F., and Boxer, D. H. (1985) *Biochemistry 24*, 40–46.

19. Giordani, R., Buc, J., Cornish-Bowden, A., and Cardenas, M. L. (1997) *Eur. J. Biochem. 250*, 567–577.

20. Rothery, R. A., Blasco, F., and Weiner, J. H. (2001) *Biochemistry 40*, 5260–5268.

21. Zhao, Z., and Weiner, J. H. (1998) *J. Biol. Chem. 273*, 20758–20763.

22. Zhao, Z., Rothery, R. A., and Weiner, J. H. (1999) *Eur. J. Biochem. 260*, 50–56.

23. Hagerhall, C., Magnitsky, S., Sled, V. D., Schroder, I., Gunsalus, R. P., Cecchini, G., and Ohnishi, T. (1999) *J. Biol. Chem. 274*, 26157–26164.

24. Hastings, S. F., Kaysser, T. M., Jiang, F., Salerno, J. C., Gennis, R. B., and Ingledew, W. J. (1998) *Eur. J. Biochem. 255*, 317–323.

25. Veselov, A. V., Osborne, J. P., Gennis, R. B., and Scholes, C. P. (2000) *Biochemistry 39*, 3169–3175.

26. Blasco, F., Nunzi, F., Pommier, J., Brasseur, R., Chippaux, M., and Giordano, G. (1992) *Mol. Microbiol. 6*, 209–219.

27. Rothery, R. A., and Weiner, J. H. (1991) *Biochemistry 30*, 8296–8305.

28. Markwell, M. A. D., Haas, S. M., Bieber, L. L., and Tolbert, N. E. (1978) *Anal. Biochem. 87*, 206–210.

29. Rothery, R. A., Chatterjee, I., Kiema, G., McDermott, M. T., and Weiner, J. H. (1998) *Biochem. J. 332 (Pt 1)*, 35–41.

30. Rao, P. S., and Hayon, E. (1973) *J. Phys. Chem. 77*, 2274–2276.

31. Patel, K. B., and Willson, R. L. (1973) *J. Chem. Soc., Faraday Trans. 1 69*, 814–825.

32. Brondijk, T. H., Fiegen, D., Richardson, D. J., and Cole, J. A. (2002) *Mol. Microbiol. 44*, 245–255.

33. Wallace, B. J., and Young, I. G. (1977) *Biochim. Biophys. Acta 461*, 84–100.

34. Strickland, S., Palmer, G., and Massey, V. (1975) *J. Biol. Chem. 250*, 4048–4052.